Journal of Photochemistry and Photobiology A: Chemistry 208 (2009) 117–124

Contents lists available at ScienceDirect

Journal of Photochemistry and Photobiology A: Chemistry

journal homepage: www.elsevier.com/locate/jphotochem

Triple fluorescence of acridinedione: Locally excited, photoinduced electron transfer promoted charge transfer and anion induced charge transfer states

P. Ashokkumar[a], V. Thiagarajan[a,b], S. Vasanthi[a], P. Ramamurthy[a,*]

[a] National Centre for Ultrafast Processes, University of Madras, Taramani Campus, Chennai 600 113, India
[b] CEA, Institut de Biologie et Technologies de Saclay (IBITECS) and CNRS, Gif-sur-Yvette, F-91191, France

ARTICLE INFO

Article history:
Received 16 July 2009
Received in revised form 22 August 2009
Accepted 3 September 2009
Available online 11 September 2009

Keywords:
Acridinedione dyes
Triple fluorescence
Heteroditopic host
Photoinduced electron transfer
Anion induced charge transfer

ABSTRACT

A dual emitting acridinedione fluorophore, 9-(4-(dimethylamino)phenyl)-3,4,6,7,9,10-hexahydroacridine-1,8(2H,5H)-dione (DMAADR-1), was synthesized and its dual fluorescence behavior was found to be greatly affected by the presence of both transition metal ions and anions. Addition of transition metal ions results in the fluorescence enhancement in the locally excited (LE) state with the disappearance of charge transfer (CT) state by suppression of photoinduced electron transfer (PET) process. Whereas in the case of anions like acetate, phosphate and fluoride, a triple fluorescence is observed, corresponding to the LE state, PET promoted CT state and anion induced CT (AICT) state. Since the present molecule can act as heteroditopic host for both transition metal ions and anions, we have carried out simultaneous binding studies of metal ions and anions. These studies clearly proved the sequestering of the ions and thus tuned the fluorescence of DMAADR-1 between OFF–ON states.

1. Introduction

The understanding of dual fluorescence of organic molecules in solution offers a challenging problem. Four decades ago, Lippert et al. [1,2] discovered the dual fluorescence behavior of 4-(N,N-dimethylamino)benzonitrile (DMABN) in polar solvents. Since then, this phenomenon has been observed for a wide range of systems of the same family as well as nonsubstituted linear polyene compounds [3]. Apart from the dual fluorescence, triple fluorescence was also observed in some compounds due to various photophysical processes. For example, triple fluorescence states were reported for DMABN in polar solvents, using time-resolved infrared (TRIR) spectral studies [4], and the peaks are assigned to the normal LE, CT state and hydrogen bonded CT state (HICT); triple fluorescence was also observed in DMABN–cyclam complex in ethanol corresponding to LE state, a twisted intramolecular charge transfer (TICT) state, and an intramolecular exciplex [5,6]; pressure induced triple fluorescence of N-salicylidine-3-hydroxy-4-(benzo[d]thiazol-2-yl)phenyl amine (SaIHBP) was reported [7] and the peaks are assigned to the emission from the enol–enol, keto–enol, enol–keto excited states of the molecule; solvent induced triple fluorescence of SaIHBP was also reported corresponding to the presence of three excited state tautomers [8]; triple fluorescence of substituted benzanilide was observed corresponding to LE state, intermolecular proton transfer between trans isomer and intramolecular charge transfer (ICT) state [9]; BF_2-chelated tetraaryl aza dipyrromethane shows triple fluorescence on the variation of acid content due to the stepwise protonation process [10].

Fluorescence OFF–ON signaling systems for various neutral and ionic analytes have attracted considerable attention due to their biological, chemical and environmental importance [11,12]. Among the various fluorescent sensors, the PET-based chemosensors are widely used and have been proven successful as direct fluorescent cation and anion sensing molecules [13–16]. Generally N or O donor centres chosen to be the cation receptors [17,18] and the hydrogen bonding donors like urea, thiourea, amide, pyrrole, imidazole, indole moieties or boron, silicon which can form Lewis adduct with anion chosen to be the anion receptor [19–23]. Simultaneous sensing of both types of charged analytes have been achieved with the use of heteroditopic host that can simultaneously bind both metal ions and anions [24–30]. Fluorescence enhancement is considered as an essential feature of a chemosensor, because it reduces the interference induced by other factors [31]. Unlike alkaline and alkaline earth metal ions, most of the transition metal ions are known as fluorescence quenchers, design of OFF–ON type fluorescent chemosensors for transition metal ion is a difficult task. There are two developed strategies to solve this problem. One is to design a proper receptor which binds the ions tighter than fluorophore does and the other one is use of electron deficient fluorophore to avoid the direct communication between the fluorophore and the transition metal ion. With all these in our mind we have designed a chemosensor with dimethylamino group as a receptor and the elec-

* Corresponding author. Tel.: +91 44 24540962; fax: +91 44 24546709.
E-mail address: prm60@hotmail.com (P. Ramamurthy).

1010-6030/$ – see front matter © 2009 Elsevier B.V. All rights reserved.
doi:10.1016/j.jphotochem.2009.09.004

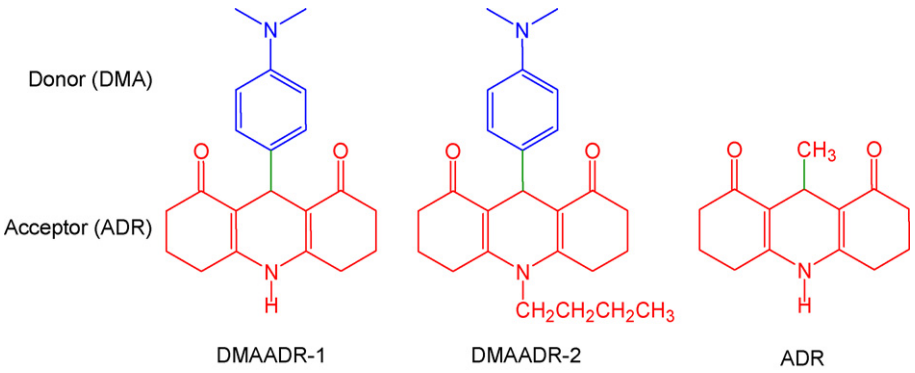

Scheme 1. Structure of acridinedione dyes.

tron deficient acridinedione as a fluorophore. In addition to this, the ring amino hydrogen serves as a good hydrogen bond donor, through which anion sensing was achieved. Since the present system consists of two distinct binding sites for the transition metal ions and anions, sensing of both types of analytes will be possible using this system.

Our interest has been in the design of fluorescent sensor molecules capable of selectively monitoring metal ions and anions using acridinedione (ADD) as a fluorophore [32–35]. Since both PET and ICT mechanism can operate in acridinedione, it will be good to use it as a signaling unit in sensor molecules. Acridinedione dyes have been reported as a laser dyes with lasing efficiency comparable to that of coumarin-102 [36–39]. The photophysical and photochemical properties of ADD dyes in solution [40,41] and PMMA matrix were extensively studied [42]. Dual emission behavior of 9-N,N-dimethylaniline decahydroacridinedione (DMAADD) has been studied and this was attributed to the presence of two different emission states, namely locally excited (LE) and PET promoted CT state [32]. Here, we report the metal ion and anion binding studies of DMAADR-1 molecule, which shows triple fluorescence in the presence of anions. To confirm the involvement of amino hydrogen in the hydrogen bonding interaction with the anions we have synthesized a reference compound with n-butyl group instead of hydrogen on the ring nitrogen atom.

2. Experimental methods

All the metal ions (as their perchlorates); anions (as their tetrabutyl ammonium salts); cyclohexanedione and 4-dimethylamino benzaldehyde were purchased from Sigma–Aldrich Chemicals Pvt. Ltd. Acetonitrile used in this investigation was of HPLC grade purchased from Qualigens India Ltd. Absorption spectra were recorded in Agilent 8453 diode array spectrophotometer. Emission spectra were recorded in PerkinElmer MPF-44B fluorescence spectrophotometer interfaced with PC through Rishcom-100 multimeter. Fluorescence decays were recorded using IBH time correlated single photon counting technique as reported elsewhere.

3. Results and discussion

In order to confirm the involvement of both the chromophores in the anomalous CT state formation, we have prepared different acridinedione derivatives (Scheme 1) with varying substitution at the donor and acceptor moiety by the methods described in the literature [38]. Absorption spectra of these dyes shows a maximum at 360 nm in acetonitrile, and this band has been assigned to the ICT from the ring nitrogen to ring carbonyl oxygen centre within the acridinedione fluorophore (Fig. S1). Presence of electron donating substituents in the 9th position (donor) did not show any change in the absorption maximum. Whereas, the presence of the same in the 10th position shows red shift due to its ICT nature. A shoulder at the shorter wavelength is observed for DMAADR dyes around 300 nm and this is assigned to the intramolecular transition within the substituted 9-aryl group (donor). In contrast to the absorption spectrum, the emission spectrum (Fig. S2) recorded by exciting the dye at its longer wavelength absorption maximum is found to depend on the electron donating property of the groups present in the 9th position. For ADR, the first excited state remains largely localised on the acridinedione itself. Whereas in DMAADR-1 and -2, the PET from the donor to the acceptor produces a low lying anomalous CT state in aprotic polar solvents as similar to our earlier report [32]. This CT state leads to the new longer wavelength fluorescence (around 570 nm) in addition to the LE state emission (around 420 nm) as observed in ADR. Emission maximum of both the states was found to be independent of excitation wavelength. However, CT/LE state intensity ratio depends on the excitation wavelength. Excitation of DMAADR-1 at 300 nm results in the larger ratio of CT/LE state intensity compared to other wavelengths as shown in Fig. S3. Since CT state originates from the dimethylamino donor moiety, excitation at its absorption wavelength leads to the stronger CT state fluorescence compared to LE state. The emission spectra of DMAADR-1 recorded in various solvents are shown in Fig. 1. In protic solvents, protonation of the dimethylamino group increases the oxidation potential of donor group, which results in the LE state fluorescence only. Substitution of n-butyl group in the 10th position (acceptor), did not show any change in the emis-

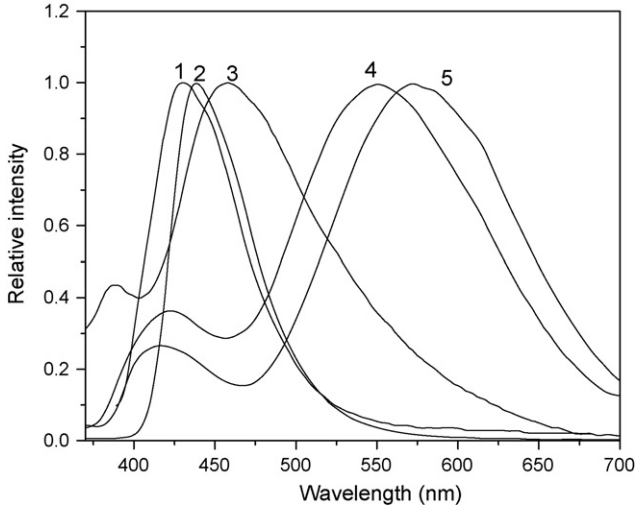

Fig. 1. Emission spectra of DMAADR-1 in different solvents (1) methanol, (2) water, (3) benzene, (4) chloroform and (5) acetonitrile.

Table 1
Fluorescence lifetime parameters of ADR, DMAADR-1 and DMAADR-2 in acetonitrile. λ_{ex} = 375 nm; preexponential factors (in parenthesis).

Dyes	Decay monitored at 420 nm			Decay monitored at 487 nm			Decay monitored at 570 nm	
	τ_1 (ns)	τ_2 (ns)	τ_3 (ns)	τ_1 (ns)	τ_2 (ns)	τ_3 (ns)	τ_1 (ns)	τ_2 (ns)
ADR	5.65	–	–	5.65	–	–	–	–
DMAADR-1	0.62 (34.58)	1.54 (65.42)	–	0.62 (71.64)	1.54 (28.36)	–	0.62	–
DMAADR-1 + Mn^{2+} [a]	2.30	–	–	2.30	–	–	2.30	–
DMAADR-1 + AcO^- [b]	0.62 (13.26)	1.54 (31.32)	6.30 (55.42)	0.62 (24.84)	1.54 (5.90)	6.30 (69.26)	0.62 (45.65)	6.30 (54.35)
DMAADR-2	0.62 (5.23)	4.06 (94.77)	–	0.62 (42.02)	4.06 (57.98)	–	0.62 (95.42)	4.06 (4.58)
DMAADR-2 + Mn^{2+} [a]	7.15	–	–	7.15	–	–	7.15	–

[a] At the limiting concentration of Mn^{2+} (Table 2).
[b] Concentration of AcO^- is 3.04 mM.

sion maximum of CT state; whereas it caused enhancement of LE state intensity compared to CT state due to the increased charge density on ring nitrogen. The above observations clearly state that both the donor and acceptor moieties of DMAADR-1 are involved in the longer wavelength anomalous CT state formation. Fluorescence decay of ADR obeys single exponential fit with the lifetime of 5.65 ns. Whereas, DMAADR dyes show biexponential decay in LE state and single exponential decay in the CT state (Table 1). The longer lifetime component is due to the PET quenched LE state and shorter lifetime component is due to the PET promoted CT state. DMAADR-1 shows lifetime of 0.62 and 1.54 ns for CT and LE state respectively. The biexponential nature of the fluorescence decay at wavelengths below 530 nm is due to the spectral overlap of the LE and CT states. Above 530 nm, only the CT state lifetime of 0.62 ns is observed. DMAADR-2 shows 0.62 and 4.06 ns for CT and LE state respectively.

3.1. Metal ion binding studies

Figs. 2 and 3 show the effect of Fe(II) on the absorption and emission spectra of DMAADR-1 in acetonitrile respectively. The disappearance of the DMA absorption around 300 nm in the presence of transition metal ions suggests the interaction of metal ions with the DMA donor group in the ground state. The corresponding emission spectra show fluorescence enhancement in the LE state accompanied with the disappearance of CT state. In the presence of the transition metal ions, the fluorophore-donor communication is turned off due to the binding of the metal ions at the donor site, thereby leading to the fluorescence enhancement in LE state and suppression of longer wavelength CT state as similar to our earlier report [32]. Full recovery of the fluorescence takes place at the limiting concentration (Table 2) of the metal ion due to the complete

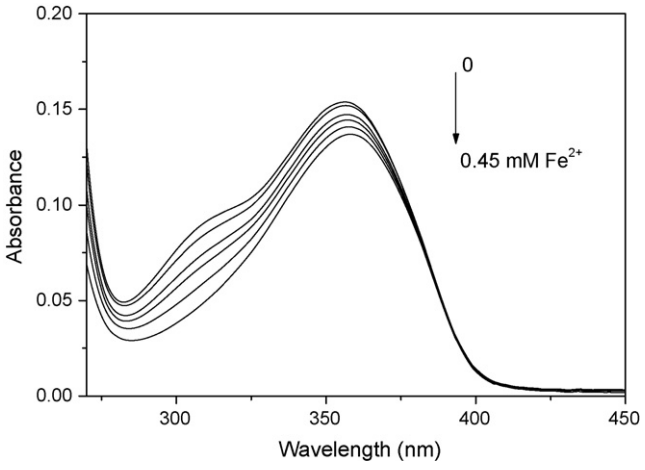

Fig. 2. Absorption spectra of DMAADR-1 (1.60×10^{-5} M) in acetonitrile upon addition of Fe^{2+} (0–0.45 mM).

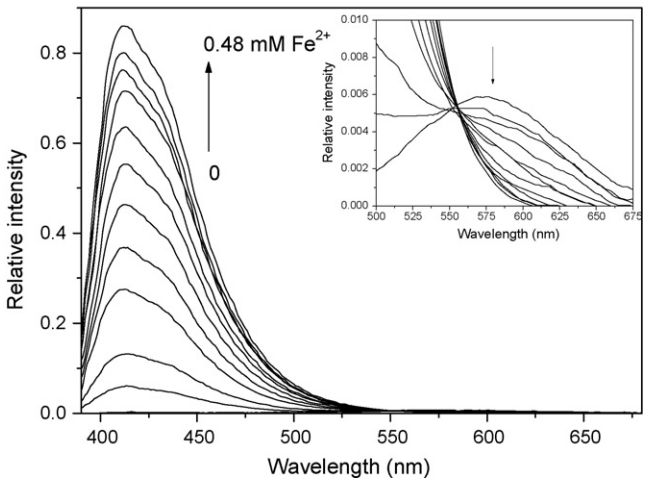

Fig. 3. Emission spectra of DMAADR-1 (1.60×10^{-5} M) in acetonitrile upon addition of Fe^{2+} (0–0.48 mM). λ_{ex} = 380 nm. Inset shows the emission spectra in the region of 500–675 nm.

suppression of PET process. The maximum fluorescence enhancement of DMAADR-1 dye for various metal ions is presented in Table 2. The fluorescence decay monitored at the LE state gradually turns from biexponential to single exponential during the addition of metal ions. Fig. 4 presents the fluorescence decays of DMAADR-1 at different concentrations of Mn^{2+} in acetonitrile. In the presence of metal ions, the CT state shorter lifetime component (0.62 ns)

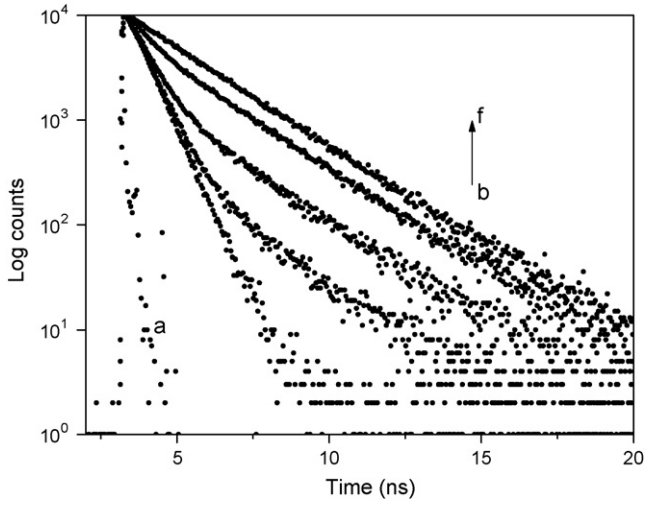

Fig. 4. Fluorescence decay profiles of DMAADR-1 (1.96×10^{-5} M) at different concentrations of Mn^{2+} in acetonitrile, λ_{ex} = 375 nm and λ_{em} = 570 nm. (a) Laser profile, (b) dye alone, (c) 0.22 mM of Mn^{2+}, (d) 0.67 mM of Mn^{2+}, (e) 1.11 mM of Mn^{2+} and (f) 1.56 mM of Mn^{2+}.

Table 2
Fluorescence output of DMAADR-1 and DMAADR-2 (1.60×10^{-5} M) in acetonitrile with different transition metal ion input. λ_{ex} = 380 nm (at isosbestic point).

Input metal ion	DMAADR-1		DMAADR-2	
	Limiting concentration of metal ion[a] [M]	Output fluorescence enhancement	Limiting concentration of metal ion[a] [M]	Output fluorescence enhancement
Mn^{II}	1.4×10^{-3}	300	1.6×10^{-3}	98
Fe^{II}	4.8×10^{-4}	430	2.4×10^{-4}	125
Co^{II}	2.8×10^{-2}	222	4.6×10^{-2}	81
Ni^{II}	1.1×10^{-3}	252	6.4×10^{-3}	86
Cu^{II}	3.7×10^{-5}	174	3.7×10^{-5}	56
Zn^{II}	1.2×10^{-3}	229	8.5×10^{-3}	85

[a] Represents the concentration of the metal ion for which fluorescence enhancement is maximum.

disappears gradually and the PET quenched LE state longer lifetime increases (1.54–2.30 ns) along with increasing amplitude. We observe a single exponential decay with longer lifetime component at the limiting concentration of metal ions.

Metal ion binding studies of DMAADR-2 also shows the similar behavior as in the case of DMAADR-1. But due to the enhanced ICT transition within the acridinedione fluorophore, it shows relatively stronger LE state fluorescence and thus the enhancement ratio with metal ions remains lower. The maximum fluorescence enhancement of DMAADR-2 dye for various metal ions is presented in Table 2.

3.2. Triple emission states in the presence of anion

Fig. 5 shows the absorption spectra of DMAADR-1 in acetonitrile in the presence of varying concentration of acetate. Addition of AcO^- shows a red shift of 14 nm (356–370 nm) along with an isosbestic point at 366 nm. A clear isosbestic point shows the existence of two states of 1:1 complex. The corresponding fluorescence spectra (Fig. 6), when excited at its isosbestic point show the formation of a new emission peak at 487 nm in addition to the normal LE and CT state emission. Whereas the addition of AcO^- to the ADR dye, which has the similar anion binding site, shows a linear decrease in the LE state (420 nm) intensity along with the formation of a new emissive ICT state around 490 nm. In the present study, dual emitting acridinedione DMAADR-1 shows a new peak corresponding to the anion induced charge transfer (AICT) in addition to the LE and CT peaks. In order to confirm the above three different emission states, 3D emission spectral studies have been performed as shown in Fig. S4. In acetonitrile, two contours at the emission wavelength of 420 and 570 nm were observed for DMAADR-1. After the addition of AcO^-, third contour at 490 nm appears with increasing intensity. This triple emission states are also confirmed by time resolved fluorescence studies. Figs. 7 and 8 show the fluorescence decay of DMAADR-1 with the addition of AcO^- when monitored at 487 and 570 nm respectively. Addition of AcO^- shows triexponential decay when monitored at 487 nm with the lifetime of

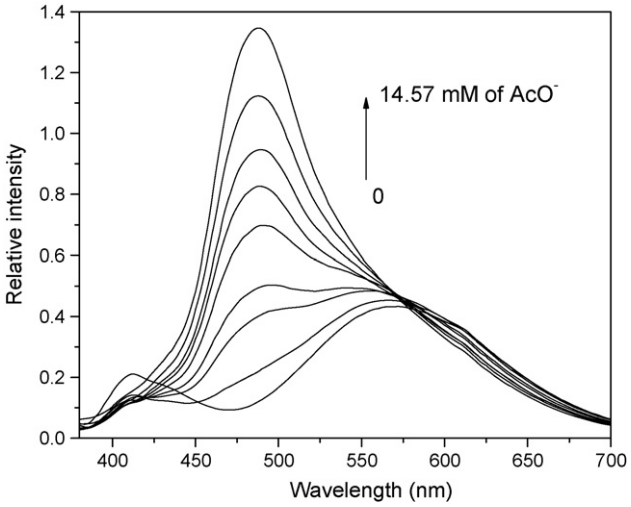

Fig. 6. Emission spectra of DMAADR-1 (2.80×10^{-5} M) in acetonitrile upon addition of AcO^- (0–14.57 mM). λ_{ex} = 366 nm.

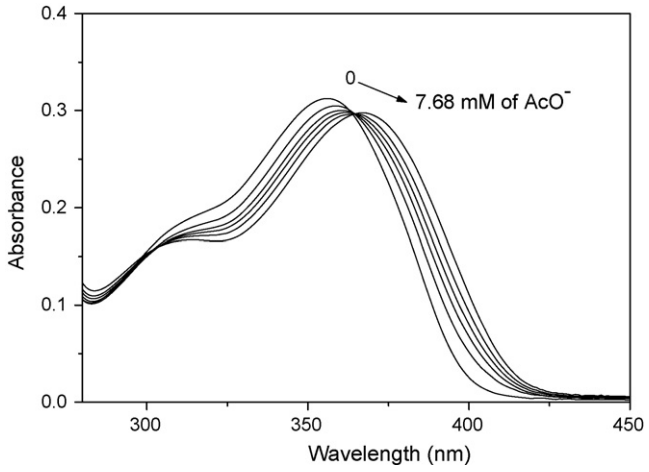

Fig. 5. Absorption spectra of DMAADR-1 (2.80×10^{-5} M) in acetonitrile upon addition of AcO^- (0–7.68 mM).

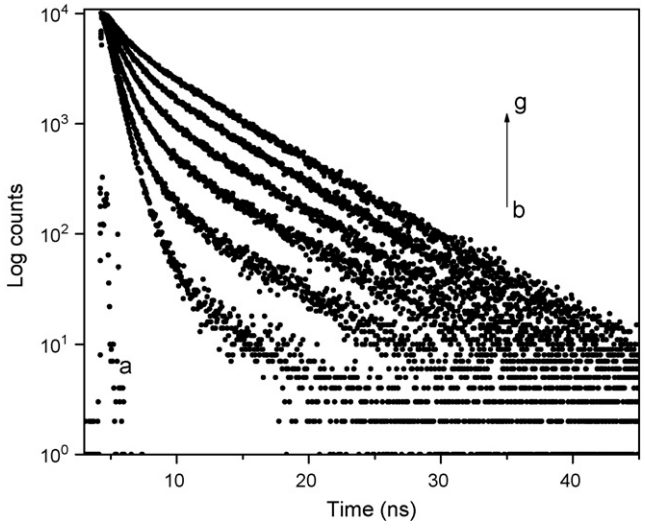

Fig. 7. Fluorescence decay profile of DMAADR-1 (2.30×10^{-5} M) at different concentrations of AcO^- in acetonitrile; λ_{ex} = 375 nm and λ_{em} = 487 nm: (a) laser profile, (b) dye alone, (c) 0.076 mM of AcO^-, (d) 0.101 mM of AcO^-, (e) 0.507 mM of AcO^-, (f) 1.013 mM of AcO^- and (g) 3.040 mM of AcO^-.

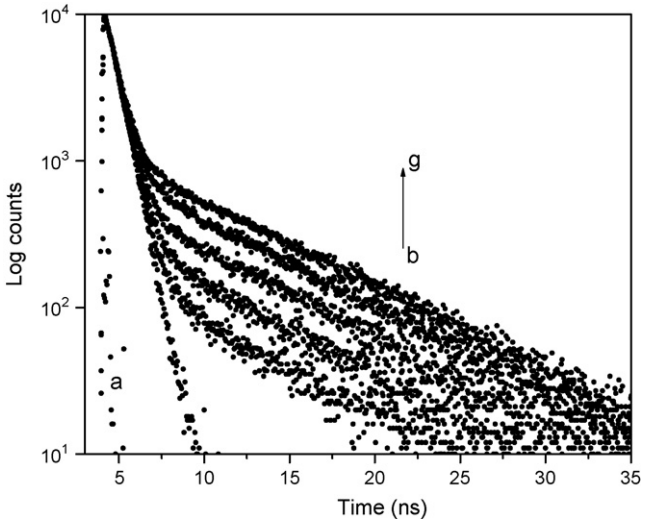

Fig. 8. Fluorescence decay profile of DMAADR-1 (2.30×10^{-5} M) at different concentrations of AcO^- in acetonitrile; λ_{ex} = 375 nm and λ_{em} = 570 nm: (a) laser profile, (b) dye alone, (c) 0.076 mM of AcO^-, (d) 0.101 mM of AcO^-, (e) 0.507 mM of AcO^-, (f) 1.013 mM of AcO^- and (g) 3.040 mM of AcO^-.

1.54 ns (LE state), 6.30 ns (AICT state) and 0.62 ns (CT state). At 570 nm, it shows biexponential decay corresponding to CT and AICT state. The CT component amplitude (0.62 ns) decreases gradually on increasing concentration of AcO^-, and the new longer component (6.30 ns) amplitude increases. These observations confirm the presence of three different emission states of the DMAADR-1 in the presence of acetate ion as shown in Scheme 2. The binding of AcO^- through hydrogen bonding at the amino hydrogen increases the electron density, thereby enhancing ICT transition in the ADR system that results in the observed red shift in the absorption maximum and the formation of new ICT peak in the emission spectral studies. Further more, the enhanced electron density in the acceptor moiety decreases reduction potential of the fluorophore and thus suppresses the PET process, which is clearly observed from the decreasing amplitude of the CT state fluorescence lifetime. Binding of metal ion at the PET donor site increases the oxidation potential of the donor and thus suppresses the PET process. In the same way, binding of anion at the PET acceptor site decreases the reduction potential of the acceptor and thus suppresses the PET process.

Addition of $H_2PO_4^-$ shows a red shift of 11 nm (356–367 nm) along with a clear isosbestic point at 363 nm (Fig. S5). The corresponding fluorescence spectra shows red shift in the LE state along with the formation of new peak around 480 nm without altering CT state (Fig. S6). The group is at present working on the theoretical studies to determine the exact conformation of anion bound DMAADR-1, which will reveal the observed red shift in the case of $H_2PO_4^-$. Addition of F^- shows a color change visible to naked eye (from colorless to an intense fluorescent green). Upon addition of F^-, the peak at 356 nm decreases while a new peak appears at 450 nm (Fig. S7) with a isosbestic point around 385 nm. The emission spectra recorded by exciting the sample at its isosbestic point show a new strong peak around 500 nm (Fig. S8). Since this peak is very strong, other two peaks namely LE and CT peaks are not clearly visible. The time resolved fluorescence studies of DMAADR-1 with $H_2PO_4^-$ and F^- also show the similar behavior as in the case of AcO^-. $H_2PO_4^-$ shows the longer lifetime of 6.58 ns and F^- shows 6.12 ns.

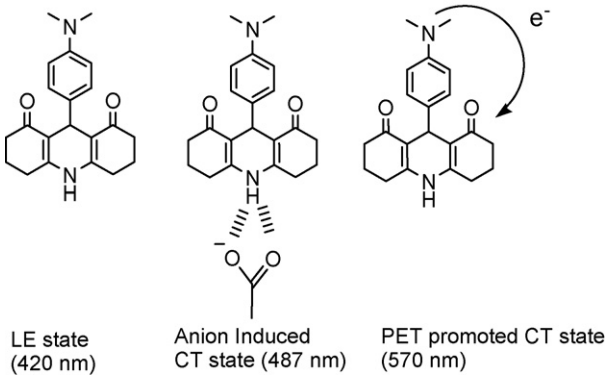

Scheme 2. Triple emission states of DMAADR-1 in the presence of AcO^-.

Addition of AcO^- and $H_2PO_4^-$ results in the in the hydrogen bonding with the amino hydrogen, whereas the addition of F^- resulted in the deprotonation, which enhances push–pull character of the ICT transition, which reflected in the visible color change and the large red shifted new emission maximum. Addition of OH^- also shows the new absorption peak around 460 nm which is due to the deprotonated form of the DMAADR moiety. The deprotonated form of the ADR dyes absorbs around 450–470 nm and emits around 500–520 nm [43]. The similar response of F^-, as in the case of OH^- confirms that $DMAADR^-$ is formed due to the deprotonation of the amino hydrogen of the DMAADR-1 moiety. The above photophysical changes mainly depend on the charge, size, electro negativity and hydrogen bond capability of the anion that reflects in the different optical output for different anions. Since F^- is smaller and having higher charge density, it results in the deprotonation, whereas AcO^- and $H_2PO_4^-$ involves in hydrogen bonding interaction. Addition of other less basic anions like Cl^-, Br^-, I^-, HSO_4^-, ClO_3^- did not show any change in the steady state and time resolved fluorescence studies.

To confirm the involvement of hydrogen bonding interaction and deprotonation, anion binding studies were carried out in DMAADR-2 which has n-butyl group instead of N–H. No significant change was observed in the absorption and emission spectral studies during the addition of all these anions. This clearly reveals that the formation of new peak in DMAADR-1 is due to the hydrogen bonding interaction in the case of AcO^- and $H_2PO_4^-$; deprotonation in the case of F^-.

3.3. Sensing in the presence of competing ions

Since the present system consists of two distinct binding sites for metal ions and anions, we examined the effect of competing anion on the binding ability of DMAADR-1 for metal ions and vice versa. First we have titrated DMAADR-1 with the acetate in the presence of Zn^{2+} (limiting concentration). The spectral changes are shown in Figs. 9 and 10. As can be seen, initial addition of AcO^- brings back the DMA absorption around 300 nm. This suggests the sequestering of metal ion from the binding site and the presence of free DMAADR-1. However, when sequestering of the metal ion is complete, further addition of AcO^- binds at the NH moiety and results in the red shift in the absorption maximum as observed in the anion binding studies. Similar results are also obtained in emission spectral studies. At the initial concentration of AcO^-, LE state emission decreases and the CT state emission enhanced; after the complete sequestering of the metal ion, AICT state emission appears with the increasing intensity. Due to the effective PET process, DMAADR-1 shows no fluorescence, which is in OFF state; addition of metal ion suppresses the PET process and switches ON the fluorescence; addition of anions to this system sequester the metal ion and switches OFF its fluorescence; further addition of anions influences ICT process and again switches ON the fluorescence. So the sequential addition of metal ions and anions switches DMAADR-1 fluorescence between OFF–ON–OFF–ON states as shown in Scheme 3.

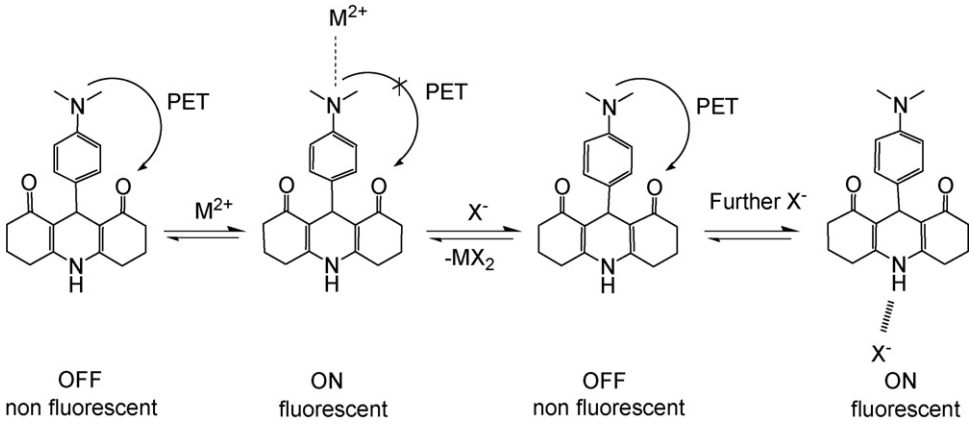

Scheme 3. Schematic representation of OFF–ON–OFF–ON fluorescence signal DMAADR-1 with the addition of competing ions.

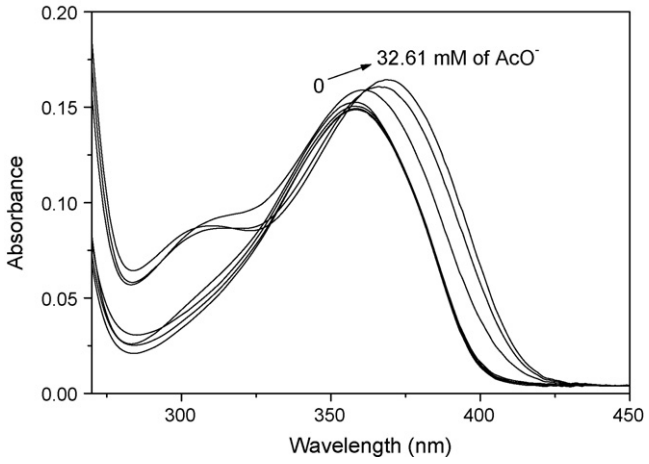

Fig. 9. Absorption spectra of DMAADR-1 (1.67×10^{-5} M) + Zn^{2+} (1.20 mM) in acetonitrile upon addition of AcO^- (0–32.61 mM).

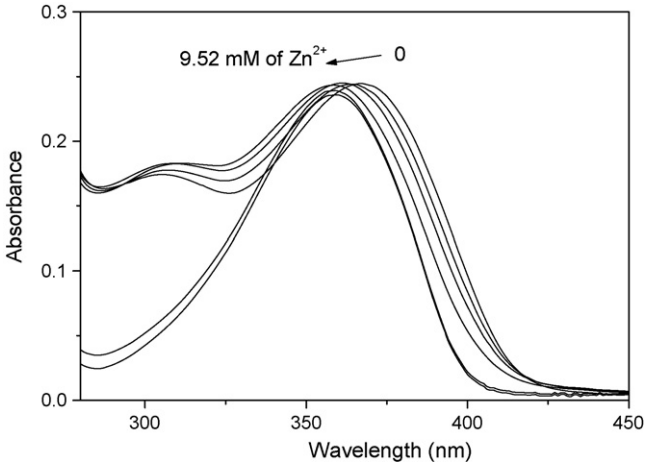

Fig. 11. Absorption spectra of DMAADR-1 (2.00×10^{-5} M) + AcO^- (17.24 mM) in acetonitrile upon addition of Zn^{2+} (0–9.52 mM).

In the second experiment Zn^{2+} was titrated with DMAADR-1 + 17.24 mM of AcO^-. Addition of Zn^{2+} results in the 14 nm blue shift of the absorption maximum and brings back the original absorption spectrum of DMAADR-1 as shown in Fig. 11. Further addition of Zn^{2+} results in the disappearance of DMA absorption around 300 nm. The corresponding emission spectra (Fig. 12) show the gradual decrease of AICT peak at the initial concentration, after that the LE state appears with increasing intensity with the disappearance of CT state emission. Time resolved fluorescence studies also confirmed the sequestering process. Even though DMAADR-1 contain distinct binding sites for both metal ions and anions, positive cooperative binding of both type analytes, as observed

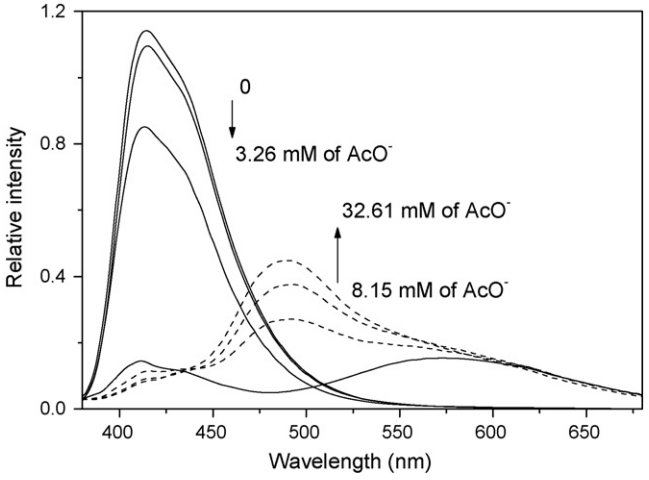

Fig. 10. Emission spectra of DMAADR-1 (1.67×10^{-5} M) + Zn^{2+} (1.20 mM) in acetonitrile upon addition of AcO^- (0–32.61 mM). λ_{ex} = 366 nm.

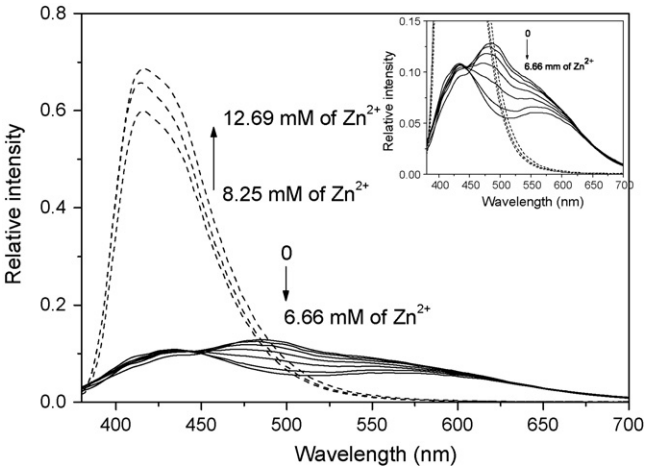

Fig. 12. Emission spectra of DMAADR-1 (2.00×10^{-5} M) + AcO^- (17.24 mM) in acetonitrile upon addition of Zn^{2+} (0–12.69 mM). λ_{ex} = 360 nm. Inset shows the expanded region of relative intensity.

exploiting the allosteric effect [44,45], through electrostatic interactions between the ion pairs [46,47] or to the host as an associated ion pair [48], is not possible in this case due to the absence of close proximity of two binding sites. We attribute this sequestering process due to the weak binding of ions to the host molecule and ion-pairing equilibria between two types of ions. In most organic solvents, the metal ions and anions do not exist as free ions, instead they are present as solvent separated ion pairs, contact ion pairs, and/or aggregated contact ion pairs [49,50]. Ion pairing with the competing ion diminishes the host–guest binding ability.

4. Conclusion

Triple emission of acridinedione was observed in the presence of anions corresponding to LE, AICT and CT state. This kind of anion induced triple fluorescence is the first of its kind. Since DMAADR-1 consist two distinct binding sites for both metal ions and anions, sensing of both types of ions were achieved using the present molecule. Binding of transition metal ion suppresses the PET process and thus enhances the fluorescence upto a maximum of 430-fold. Simultaneous binding studies of metal ions and anions show the sequestering of ions from the binding site and form an ion pair with the added ion. Due to the sequestering process of ions, we can effectively tune the fluorescence of DMAADR-1 by the simple addition of metal ions and anions. In a nutshell this bichromophore shows "OFF–ON–OFF–ON" fluorescence in the sequential addition of metal ions and anions.

Acknowledgement

We thank the Department of Science and Technology, Government of India, for financial support (DST/SR/S1/PC-31/2005).

Appendix A. Supplementary data

Supplementary data associated with this article can be found, in the online version, at doi:10.1016/j.jphotochem.2009.09.004.

References

[1] E. Lippert, W. Luder, F. Moll, H. Nagele, H. Boos, H. Prigge, I. Siebold-Blankenstein, Umwandlung von Elektronenanregungsenergie, Angew. Chem. 73 (1961) 695–706.
[2] E. Lippert, W. Luder, H. Boos, in: A. Mangini (Ed.), Advances in Molecular Spectroscopy, Pergamon Press, Oxford, UK, 1962, p. 443.
[3] Z.R. Grabowski, K. Rotkiewicz, W. Rettig, Structural changes accompanying intramolecular electron transfer: focus on twisted intramolecular charge-transfer states and structures, Chem. Rev. 103 (2003) 3899–4032.
[4] W.M. Kwok, M.W. George, D.C. Grills, C. Ma, P. Matousek, A.W. Parker, D. Phillips, W.T. Toner, M. Towrie, Direct observation of a hydrogen-bonded charge-transfer state of 4-dimethylaminobenzonitrile in methanol by time-resolved IR spectroscopy, Angew. Chem. Int. Ed. 42 (2003) 1826–1830.
[5] L.S. Choi, G.E. Collins, Triple fluorescence of 4-(1,4,8,11-tetraazacyclotetradecyl)benzonitrile, Chem. Commun. (1998) 893–894.
[6] G.E. Collins, L.S. Choi, J.H. Callahan, Effect of solvent polarity, pH, and metal complexation on the triple fluorescence of 4-(N-1,4,8,11-tetraazacyclotetradecyl)benzonitrile, J. Am. Chem. Soc. 120 (1998) 1474–1478.
[7] S. Li, Q. Wang, Y. Qian, S. Wang, Y. Li, G. Yang, Understanding the pressure-induced emission enhancement for triple fluorescent compound with excited-state intramolecular proton transfer, J. Phys. Chem. A 111 (2007) 11793–11800.
[8] W. Sun, S. Li, R. Hu, Y. Qian, S. Wang, G. Yang, Understanding solvent effects on luminescent properties of a triple fluorescent ESIPT compound and application for white light emission, J. Phys. Chem. A 113 (2009) 5888–5895.
[9] S. Lucht, J. Stumpe, M. Rutloh, Triple fluorescence of substituted benzanilides in solution and in solid states, J. Fluoresc. 8 (1998) 153–166.
[10] S.O. McDonnell, D.F. O'Shea, Near-infrared sensing properties of dimethlyamino-substituted BF_2-azadipyrromethenes, Org. Lett. 8 (2006) 3493–3496.
[11] J.P. Desvergne, A.W. Czarnik, Chemosensors of Ion and Molecule Recognition, Kluwer, Dordrecht, 1997.
[12] B. Valeur, I. Leray, Design principles of fluorescent molecular sensors for cation recognition, Coord. Chem. Rev. 205 (2000) 3–40.
[13] A.P. de Silva, H.Q.N. Gunaratne, T. Gunnlaugsson, A.J.M. Huxley, C.P. McCoy, J.T. Rademacher, T.E. Rice, Signaling recognition events with fluorescent sensors and switches, Chem. Rev. 97 (1997) 1515–1566.
[14] S.K. Kim, J. Yoon, A new fluorescent PET chemosensor for fluoride ions, Chem. Commun. (2002) 770–771.
[15] T. Gunnlaugsson, A.P. Davis, J.E. O'Brien, M. Glynn, Fluorescent sensing of pyrophosphate and bis-carboxylates with charge neutral PET chemosensors, Org. Lett. 4 (2002) 2449–2452.
[16] S.C. Burdette, G.K. Walkup, B. Spingler, R.Y. Tsien, S.J. Lippard, Fluorescent sensors for Zn^{2+} based on a fluorescein platform: synthesis, properties and intracellular distribution, J. Am. Chem. Soc. 123 (2001) 7831–7841.
[17] V. Balzani, A. Juris, M. Venturi, S. Campagna, S. Serroni, Luminescent and redox-active polynuclear transition metal complexes, Chem. Rev. 96 (1996) 759–834.
[18] P. Jiang, Z. Guo, Fluorescent detection of zinc in biological systems: recent development on the design of chemosensors and biosensors, Coord. Chem. Rev. 248 (2004) 205–229.
[19] P.D. Beer, P.A. Gale, Anion recognition and sensing: the state of the art and future perspectives, Angew. Chem. Int. Ed. 40 (2001) 486–516.
[20] C. Caltagirone, P.A. Gale, Anion receptor chemistry: highlights from 2007, Chem. Soc. Rev. 38 (2009) 520–563.
[21] D.E. Gomez, L. Fabbrizzi, M. Licchelli, E. Monzani, Urea vs. thiourea in anion recognition, Org. Biomol. Chem. 3 (2005) 1495–1500.
[22] P.A. Gale, Amidopyrroles: from anion receptors to membrane transport agents, Chem. Commun. (2005) 3761–3772.
[23] K. Chellappan, N.J. Singh, I.C. Hwang, J.W. Lee, K.S. Kim, A calix[4]imidazolium[2]pyridine as an anion receptor, Angew. Chem. Int. Ed. 44 (2005) 2899–2903.
[24] M.M.G. Antonisse, D.N. Reinhoudt, Neutral anion receptors: design and application, Chem. Commun. (1998) 443–448.
[25] M.J. Deetz, M. Shang, B.D. Smith, A macrobicyclic receptor with versatile recognition properties: simultaneous binding of an ion pair and selective complexation of dimethylsulfoxide, J. Am. Chem. Soc. 122 (2000) 6201–6207.
[26] G.J. Kirkovits, J.A. Shriver, P.A. Gale, J.L. Sessler, Synthetic ditopic receptors, J. Inclusion Phenom. Macrocyclic Chem. 41 (2001) 69–75.
[27] P.A. Gale, Anion and ion-pair receptor chemistry: highlights from 2000 and 2001, Coord. Chem. Rev. 240 (2003) 191–221.
[28] J.M. Mahoney, K.A. Stucker, H. Jiang, I. Carmichael, N.R. Brinkmann, A.M. Beatty, B.C. Noll, B.D. Smith, Molecular recognition of trigonal oxyanions using a ditopic salt receptor: evidence for anisotropic shielding surface around nitrate anion, J. Am. Chem. Soc. 127 (2005) 2922–2928.
[29] J.L. Sessler, S.K. Kim, D.E. Gross, C.-H. Lee, J.S. Kim, V.M. Lynch, Crown-6-calix[4]arene-capped calix[4]pyrrole: an ion-pair receptor for solvent-separated CsF ions, J. Am. Chem. Soc. 130 (2008) 13162–13166.
[30] T. Ghosh, B.G. Maiya, A. Samanta, A colorimetric chemosensor for both fluoride and transition metal ions based on dipyrrolyl derivative, Dalton Trans. (2006) 795–801.
[31] A.W. Czarnik, Chemical communication in water using fluorescent chemosensors, Acc. Chem. Res. 27 (1994) 302–308.
[32] V. Thiagarajan, C. Selvaraju, E.J. Padmamalar, P. Ramamurthy, A novel fluorophore with dual fluorescence: local excited state and photoinduced electron-transfer-promoted charge-transfer state, Chem. Phys. Chem. 5 (2004) 1200–1209.
[33] V. Thiagarajan, P. Ramamurthy, D. Thirumalai, V.T. Ramakrishnan, A novel colorimetric and fluorescent chemosensor for anions involving PET and ICT pathways, Org. Lett. 7 (2005) 657–660.
[34] V. Thiagarajan, P. Ramamurthy, Fluorescent sensing of anions with acridinedione based neutral PET chemosensor, Spectrochim. Acta A 67 (2007) 772–777.
[35] V. Thiagarajan, P. Ramamurthy, Specific optical signalling of anions via intramolecular charge transfer pathway based on acridinedione fluorophore, J. Lumin. 126 (2007) 886–892.
[36] P. Shanmugasundaram, P. Murugan, V.T. Ramakrishnan, N. Srividya, P. Ramamurthy, Synthesis of acridinedione derivatives as laser dyes, Heteroatom Chem. 7 (1996) 17–22.
[37] P. Murugan, P. Shanmugasundaram, V.T. Ramakrishnan, B. Venkatachalapathy, N. Srividya, P. Ramamurthy, K. Gunasekaran, D. Velmurugan, Synthesis and laser properties of 9-alkyl-3,3,6,6-tetramethyl-1,2,3,4,5,6,7,8,9,10-decahydroacridine-1,8-dione derivatives, J. Chem. Soc. Perkin Trans. 2 (1998) 999–1004.
[38] N. Srividya, P. Ramamurthy, P. Shanmugasundaram, V.T. Ramakrishnan, Synthesis, characterization, and electrochemistry of some acridine-1,8-dione dyes, J. Org. Chem. 61 (1996) 5083–5089.
[39] C. Selvaraju, P. Ramamurthy, Excited-state behavior and photoionization of 1,8-acridinedione dyes in micelles—comparison with NADH oxidation, Chem. Eur. J. 10 (2004) 2253–2262.
[40] N. Srividya, P. Ramamurthy, V.T. Ramakrishnan, Photophysical studies of acridine(1,8)dione dyes: a new class of laser dyes, Spectrochim. Acta A 54 (1998) 245–253.
[41] N. Srividya, P. Ramamurthy, V.T. Ramakrishnan, Photooxidation of acridine(1,8)dione dyes: flash photolysis investigation of the mechanistic details, Phys. Chem. Chem. Phys. 2 (2000) 5120–5126.
[42] V. Thiagarajan, C. Selvaraju, P. Ramamurthy, Excited state behaviour of acridinedione dyes in PMMA matrix: inhomogeneous broadening and enhancement of triplet, J. Photochem. Photobiol. A: Chem. 157 (2003) 23–31.

[43] B. Venkatachalapathy, P. Ramamurthy, V.T. Ramakrishnan, Ground and excited states acid-base properties of acridine-1,8-dione dyes, J. Photochem. Photobiol. A: Chem. 111 (1997) 163–169.
[44] P.D. Beer, P.K. Hopkins, J.D. McKinney, Cooperative halide, perrhenate anion-sodium cation binding and pertechnetate extraction and transport by a novel tripodal tris(amido benzo-15-crown-5) ligand, Chem. Commun. (1999) 1253–1254.
[45] A. Arduini, G. Giorgi, A. Pochini, A. Secchi, F. Ugozzoli, Anion allosteric effect in the recognition of tetramethylammonium salts by calix[4]arene cone conformers, J. Org. Chem. 66 (2001) 8302–8308.
[46] S. Kubik, R. Goddard, A new cyclic pseudopeptide composed of L-proline and 3-aminobenzoic acid subunits as a ditopic receptor for the simultaneous complexation of cations and anions, J. Org. Chem. 64 (1999) 9475–9486.
[47] T. Tozawa, Y. Misawa, S. Tokita, Y. Kubo, A regioselectively bis(thiourea)-substituted dibenzo-diaza-30-crown-10: a new strategy for the development of multi-site receptors, Tetrahedron Lett. 41 (2000) 5219–5223.
[48] R. Shukla, T. Kida, B.D. Smith, Effect of competing alkali metal cations on neutral host's anion binding ability, Org. Lett. 2 (2000) 3099–3102.
[49] M. Swarc (Ed.), Ions and Ion Pairs in Organic Reactions, Wiley, New York, 1972.
[50] M.J. Kaufman, A. Streitwieser, Carbon acidity. 72. Ion pair acidities of phenyl alkyl ketones. Aggregation effects in ion pair acidities, J. Am. Chem. Soc. 109 (1987) 6092–6097.